Electrospray Ionization Ion Mobility Spectrometry of Carboxylate Anions: Ion Mobilities and a Mass−Mobility Correlation

Hugh I. Kim,[†] Paul V. Johnson,*[,‡] Luther W. Beegle,[‡] J. L. Beauchamp,[†] and Isik Kanik[‡]

Noyes Laboratory of Chemical Physics, California Institute of Technology, Pasadena, California 91125 and Jet Propulsion Laboratory, California Institute of Technology, Pasadena, California 91109-8099

Received: March 11, 2005; In Final Form: June 21, 2005

A number of carboxylate anions spanning a mass range of 87−253 amu (pyruvate, oxalate, malonate, maleate, succinate, malate, tartarate, glutarate, adipate, phthalate, citrate, gluconate, 1,2,4-benzenetricarboxylate, and 1,2,4,5-benzenetetracarboxylate) were investigated using electrospray ionization ion mobility spectrometry. Measured ion mobilities demonstrated a high correlation between mass and mobility in both N_2 and CO_2 drift gases. Such a strong mass−mobility correlation among structurally dissimilar ions suggests that the carboxylate functional group that these ions have in common is the source of the correlation. Computational analysis was performed to determine the most stable conformation of the studied carboxylate anions in the gas phase under the current experimental conditions. This analysis indicated that the most stable conformations for multicarboxylate anions included intramolecular hydrogen-bonded ring structures formed between the carboxylate group and the neutral carboxyl group. The carboxylate anions that form ring confirmations generally show higher ion mobility values than those that form extended conformations. This is the first observation of intramolecular hydrogen-bonded ring conformation of carboxylate anions in the gas phase at atmospheric pressure.

1. Introduction

An important scientific objective of future missions to Mars will be to further the search for organic molecules. The inventory of organic molecules present on the surface and subsurface can be evidence of Mars' potential for harboring either extinct or extant life. In the only search for organics on Mars to date, the two Viking landers fed regolith samples into a pyrolysis oven that heated the material to 230, 350, and 500 °C. The released volatile material was introduced into a gas chromatograph-mass spectrometer (GC-MS) for detection and identification. This analysis detected no organic material in the unconsolidated regolith analyzed at either Viking landing site.[1,2] This result was especially surprising given that $\sim 2 \times 10^5$ kg of reduced carbon is deposited on Mars each year through meteoric sources as well as through the accumulation of interplanetary dust particles.[3] Many forms of carbon found in these sources should have easily been detected given the capabilities of the Viking GC-MS.[4,5] The lack of detection has been attributed to the oxidizing conditions on the surface of Mars, which converts organics into carbon dioxide. However, recent work indicates that some complex organic material, namely the benzenecarboxylates, can be generated by oxidation of organic matter delivered to Mars by exogenic sources. This material could exist in the upper 1 m of the Martian surface in concentrations of as much as 500 parts per million (ppm) by weight.[6] Furthermore, these molecules are not volatile at 500 °C and would therefore not have been detected by the Viking GC-MS experiments.

Carboxylic acids are vital to the basic functions of terrestrial biology. If life started on Mars, it may have utilized the same underlying chemistry. As such, the discovery and identification of carboxylic acids could help identify potential biological habitats, especially if the subsurface (>1 m) is accessed on future missions. However, there is little reason to believe that Martian life would use the exact same molecules that terrestrial life would. Therefore, any systematic search for these molecules must be able to not only detect but also properly identify all types of organic molecules, not just those present in terrestrial life and in meteoritic material.

The application of electrospray ionization ion mobility spectroscopy (ESI−IMS) as a tool for the in situ detection of amino acids and peptides has been examined previously.[7−9] In particular, Johnson et al.[9] have suggested that a tandem IMS-mass spectrometer instrument (IMS-MS) could be of value in analyzing unknown samples within a complex chemical environment such as the Martian surface. Specifically, it was suggested that a tandem measurement of both an ion's mobility and mass could be used to identify unknown compounds on the basis of correlations between mass and mobility within *families* of compounds.

Griffin et al.[10] have shown that, within a collection of structurally unrelated compounds, mass and mobility are only correlated on the order of 20%. Further, they demonstrated that such correlations can be improved by an order of magnitude (2%) when only structurally related compounds are considered. Such strong mass−mobility correlations have been demonstrated through experimental and modeling efforts for a number of compound classifications, including acetyls, aromatic amines, and aliphatic amines drifting in He, N_2, air, Ar, CO_2, and SF_6[11,12] as well as for amino acids drifting in N_2 and CO_2.[9] The correlation observed among amino acids is somewhat surprising because of the large variation in molecular structure encompassed within this classification. This led Johnson et al.[9] to argue

* Author to whom correspondence should be addressed: E-mail: Paul.V.Johnson@jpl.nasa.gov.
[†] Noyes Laboratory of Chemical Physics.
[‡] Jet Propulsion Laboratory.

10.1021/jp051274h CCC: $30.25
Published on Web 08/11/2005

TABLE 1: Experimental Parameters

experimental parameter	value
temperature, K	500
drift gas flow rate (N_2/CO_2), mL/min	800/1100
electric field strength (N_2/CO_2), V/cm	280/591
E/N (N_2/CO_2), Td	1.9/4.0
cooling gas flow rate, mL/min	150
drift length, cm	13.5
ESI flow rate, μL/min	5

that strong mass−mobility correlations exist among ions with similar charge-holding structures.

As part of an effort to further explore the utility of IMS in the identification of organic compounds, as well as to better understand the origin of strong correlations among seemingly dissimilar compounds, reduced ion mobilities have been measured for a number of carboxylate anions drifting in N_2 and CO_2. In addition, a (12, 4) hard core potential model for the ion−neutral interaction has been applied to measured data sets to help evaluate the degree of the carboxylate anion mass−mobility correlation and to extract details of the ion−neutral interaction. Further, computational modeling of the ion structures was performed in order to evaluate possible origins of observed mass−mobility correlations.

2. Experimental Section

All the compounds studied in this work were purchased from Sigma Chemical Company (St. Louis, MO) and were used without further purification. All solvents (water and methanol) were HPLC grade and were purchased from J. T. Baker (Phillipsburgh, NJ). All carboxylate samples were prepared by weighing out known quantities of either carboxylic acids or their sodium salts and then dissolving them in a solvent consisting of 50% water and 50% methanol by volume to give sample concentrations of one part per thousand (ppt) by weight. Samples were then stored at 5 °C in a refrigerator until measurements were made. Prior to each measurement, samples were diluted with the solvent (50% water/50% methanol) to a concentration of 50 parts per million (ppm) by weight. This corresponds to 200−600 μM for the compounds studied.

The ESI−IMS instrument and the data acquisition system used in this investigation were based on designs previously described by Hill and co-workers[13,14] and have been described in detail by Johnson et al.[9] Throughout the course of this work, the operating conditions of the ESI−IMS instrument were virtually identical to those employed by Johnson et al.,[9] with the exception that the current measurements were made in the negative mode. An accounting of the important experimental parameters is provided in Table 1.

Throughout this work, it was assumed that ESI of the prepared samples resulted in singly charged, deprotonated carboxylate anions. Because the experiments were conducted with the drift cell at 500 K, it was further assumed that there was no significant cluster formation. These assumptions were validated through a comparison of ESI−IMS and ESI−MS spectra, which is described in detail in Section 5. A list of all organic acid anions that were investigated throughout the course of this study is given in Table 2.

As indicated in Table 1, the current experiments were conducted with electric field strengths of 280 V/cm and 591 V/cm within the drift tube when using counter-flowing preheated N_2 and CO_2 drift gases, respectively. The field strength employed in the N_2 measurements was well within the commonly accepted low field range where ion mobility is independent of the electric field (i.e., the electric field, E, to gas density, N, ratio was 1.9 Td).[15,16] However, ions drifting in CO_2 demonstrated significantly lower mobilities than in N_2. Therefore, a larger field strength was employed in order to bring the ion drift times on the same order as those seen in N_2. To ensure that the spectrometer was operating under low field conditions for carboxylate anions during the CO_2 drift gas measurements, a series of tests were conducted. Reduced mobilities were determined for maleate, phthalate, and 1,2,4-benzenetricarboxylate with electric field strengths of 591 V/cm and 325 V/cm. Agreement was seen between all corresponding mobilities within experimental uncertainties (~5%) with a maximum observed deviation of 2%. These results verified that the current measurements in CO_2 were made at sufficiently low electric fields to avoid any dependence of the measured mobilities on the electric field. In other words, the spectrometer was indeed operating under low field conditions throughout the course of this investigation.

TABLE 2: Organic Acid Anions Studied in the Present Paper

	organic acid anion	chemical formula	MW[a]
1	pyruvate[b]	$C_3H_3O_3^-$	87
2	oxalate[b]	$C_2H_1O_4^-$	89
3	malonate[b]	$C_3H_3O_4^-$	103
4	serine anion[c]	$C_3H_6NO_3^-$	104
5	maleate[b]	$C_4H_3O_4^-$	115
6	succinate[b]	$C_4H_5O_4^-$	117
7	glutarate[b]	$C_5H_7O_4^-$	131
8	aspartic acid anion[c]	$C_4H_6NO_4^-$	132
9	malate[b]	$C_4H_5O_5^-$	133
10	adipate[b]	$C_6H_9O_4^-$	145
11	glutamic acid anion[c]	$C_5H_8NO_4^-$	146
12	tartarate[b]	$C_4H_5O_6^-$	149
13	phthalate[b]	$C_8H_5O_4^-$	165
14	ascorbate[d]	$C_6H_7O_6^-$	175
15	citrate[b]	$C_6H_7O_7^-$	191
16	gluconate[b]	$C_6H_{11}O_7^-$	195
17	1,2,4-benzenetricarboxylate[b]	$C_9H_5O_6^-$	209
18	1,2,4,5-benzenetetracarboxylate[b]	$C_{10}H_5O_8^-$	253

[a] Molecular weight (amu). [b] Carboxylate anion. [c] Amino acid anion. [d] L-3-ketothreohexuronic acid (Vitamin C) anion.

Reduced ion mobilities, K_0, were determined from the recorded spectra and the experimental parameters according to the usual relation,

$$K_0 = \left(\frac{273\ \mathrm{K}}{T}\right)\left(\frac{P}{760\ \mathrm{Torr}}\right)\frac{L^2}{Vt} \qquad (1)$$

where V is the voltage drop across the drift region, L is the drift length, t is the drift time, P is the pressure and T is the temperature. With the above parameters expressed in units of V, cm, s, Torr, and K, respectively, eq 1 gave the reduced mobility in the typical units of $cm^2\ V^{-1}\ s^{-1}$. To confirm the accuracy of the present instrumentation and methodology, the reduced mobilities of three amino acids (serine, aspartic acid, and glutamic acid) drifting in N_2 were determined in positive mode and were compared with previously reported mobilities.[7,9] These comparisons showed agreement within experimental uncertainties.

3. Modeling: Theoretical Approach and Fitting Procedure

The model and fitting procedure applied to the mobility data has been described in detail by Johnson et al.[9] Therefore, only a brief description is given here. Gas-phase ion transport in the presence of an electric field (under low field conditions) is

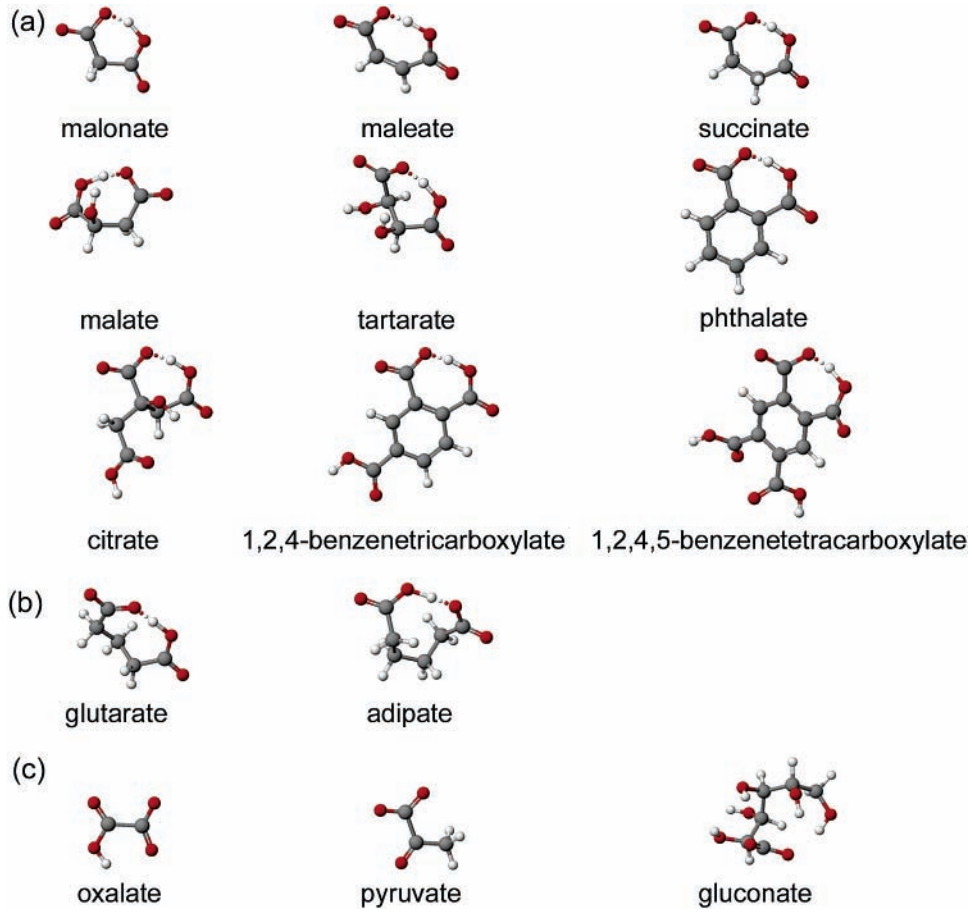

Figure 1. The most energetically favorable conformations of the studied carboxylates: (a) planar-ring conformations, (b) nonplanar-ring conformations, and (c) extended conformations.

governed by the relation,[17]

$$K = \frac{3q}{16N}\left(\frac{2\pi}{\mu kT}\right)^{1/2}\frac{1}{\Omega} \tag{2}$$

where N is the number density of the drift gas molecules, q is the charge on the ion, μ is the reduced mass, k is the Boltzmann constant, T is the temperature in the drift region, and Ω is the collision cross section. Equation 2 indicates that differences in the mobilities of ions drifting under identical conditions (i.e., temperature, pressure) are a result of the explicit mass dependence in μ and the collision cross section. The collision cross section contains all the information regarding the nature of the ion−neutral interaction and can be expressed as

$$\Omega = \pi r_m{}^2 \Omega^{(1,1)^*} \tag{3}$$

where $\Omega(1,1)^*$ is the dimensionless collision integral, which can be calculated as a function of temperature through successive integrations over collision trajectories, impact parameters, and energy.[18]

As demonstrated on a number of occasions,[9,11,12,19,20] the so-called (12, 4) hard core potential can be used to model the ion−neutral interaction. The potential is expressed as

$$V(r) = \frac{\epsilon}{2}\left\{\left(\frac{r_m - a}{r - a}\right)^{12} - 3\left(\frac{r_m - a}{r - a}\right)^{4}\right\} \tag{4}$$

where ϵ is the depth of the potential well, r is the separation between the geometric centers of the ion and neutral, r_m is the value of r at the potential minimum, and a is the location of the ionic center of charge measured from the geometrical center of the ion (see Johnson et al.[9] Figure 1). By requiring that the coefficient of the r^{-4} term equal the known polarization potential coefficient,[18] the potential depth can be set as

$$\epsilon = \frac{q^2\alpha}{3r_m^4(1 - a^*)^4} \tag{5}$$

where q is the ionic charge, α is the neutral polarizability, and the dimensionless parameter $a^* = a/r_m$ has been introduced. Tabulations of $\Omega^{(1,1)^*}$ can be found in the literature[18] for the (12, 4) hard core potential as functions of a^* and the dimensionless temperature, T^*, given by

$$T^* = \frac{kT}{\epsilon} = \frac{3kTr_m^4(1 - a^*)^4}{q^2\alpha} \tag{6}$$

If the ions and neutral molecules are represented as spherical volumes of uniform mass, then their radii are proportional to the cubed root of their masses, and r_m can be expressed as

$$r_m = (r_0 + m\gamma)\left[1 + \left(\frac{m}{M}\right)^{1/3}\right] \tag{7}$$

where a mass-dependent correction term, $m\gamma$, has been included.[11]

Rearrangement of eq 1, along with the substitution of the appropriate constants, yields

$$K_0^{-1} = (1.697 \times 10^{-4})(\mu T)^{1/2} r_m{}^2 \Omega^{(1,1)^*} \tag{8}$$

TABLE 3: Drift Times and Reduced Mobilities of Carboxylate Anions in N_2 and CO_2 Drift Gasses

	N_2		CO_2	
carboxylate anion	DT[a]	K_0[b]	DT[a]	K_0[b]
pyruvate[c]	12.96	1.97		
oxalate[c]	11.94	2.14	10.8	1.11
malonate[d]	12.93	1.97	11.4	1.05
maleate[c]	13.35	1.91	11.55	1.04
succinate[d]	13.95	1.83		
malate[c]	14.16	1.80	12.09	0.99
tartarate[c]	14.64	1.74	12.27	0.973
glutarate[c]	14.88	1.71		
adipate[c]	15.71	1.62		
phthalate[c]	15.9	1.60	12.96	0.925
citrate[c]	16.44	1.55	13.44	0.891
gluconate[d]	17.25	1.48		
1,2,4-benzenetricarboxylate[c]	17.64	1.45	1	0.836
1,2,4,5-benzenetetracarboxylate[c]	18.00	1.32	0.38	

[a] Drift time (ms). [b] Reduced mobility ($cm^2\ V^{-1}\ s^{-1}$). [c] Derived from corresponding carboxylic acid. [d] Derived from corresponding sodium carboxylate salt.

which gives the reduced ion mobility in units of $cm^2\ V^{-1}\ s^{-1}$, with r_m in Å (eq 7; calculated with r_0 in Å, m and M in amu, and γ in units of Å/amu).

Equation 8 was fit to each available data set of carboxylate ion mobility in N_2 and CO_2 using a nonlinear least-squares fitting procedure as described by Johnson et al.[9] For singly charged, deprotonated carboxylate anions, q was taken to be $e = -1.6 \times 10^{-19}$ C.

4. Computational Method

The most stable conformation for each singly charged carboxylate ion was determined through three stages of calculation using CAChe 6.1.10 (Fujitsu, Beaverton, OR). Possible molecular conformations and their corresponding potential energy maps were determined at the augmented MM3 level. Then, with the least energetic molecular conformation identified in this procedure, the geometry was optimized using the MOPAC algorithm at the PM5 level. For carboxylate anions that contain additional carboxyl or hydroxyl groups, it is possible for hydrogen bonds to form between these neutral groups and the charged carboxylate functional groups and thereby create cyclic structures. To examine the relative stability of these structures, further calculations were performed. Specifically, potential hydrogen bonds were assigned between oxygen atoms in the carboxylate functional groups and the hydrogen atoms found in nearby carboxyl or hydroxyl groups, within the previously optimized geometries. For each assigned hydrogen bond, the geometry was once again optimized using the MOPAC PM5 algorithm. Calculated heats of formation were compared between the optimized geometries determined with and without assigned hydrogen bonds. For each ion considered here, the conformation corresponding to the lowest heat of formation was taken to be the most stable. These conformations are depicted in Figure 1.

5. Results and Discussion

The drift times of singly charged carboxylate anions were determined from the locations of the peak maxima identified in the measured negative mode IMS spectra. All measured drift times and the subsequent reduced ion mobilities are listed in Table 3. Of the eleven carboxylic acid and three sodium carboxylate salt samples studied, all fourteen carboxylate anions were detected using N_2 as the drift gas, while only nine carboxylate anions were detected when CO_2 was used as the drift gas. It is unclear why some carboxylates were not detected in the CO_2 drift gas.

To confirm that the ions detected in the ESI−IMS spectra were in fact singly charged carboxylate anions, ESI−MS spectra were measured using a Finnigan LCQ Deca ion trap mass spectrometer with the entrance capillary heated to 500 K. Most of the carboxylate anions studied in this paper showed dominant peaks corresponding to singly deprotonated carboxylate anions with no evidence of multiply charged anions. However, some of the low-mass (87−117 amu) carboxylate anions (oxalate, malonate, and succinate) showed peaks of sodiated carboxylate clusters dominating the mass spectra. Therefore, IMS spectra were taken of these carboxylates with the spectrometer set to view the extended drift times expected for heavy clusters, i.e., 0−100 ms. In these spectra, only single ion peaks were observed in all but one instance, which is discussed in the following paragraph. Further, the drift times of these single peaks were comparable to other carboxylates that did not form clusters in the measured mass spectra. These observations indicate that there was no significant cluster formation in the current ESI−IMS experiments. Thus, it was assumed that the ion peak observed in the current ESI−IMS spectra were due to singly deprotonated carboxylate anions.

In the case of 1,2,4,5-benzenetetracarboxylate, two peaks were observed in the N_2−IMS spectra, one strong and one weak feature corresponding to reduced mobilities of 1.43 and 1.32 $cm^2\ V^{-1}\ s^{-1}$, respectively. When compared to the reduced ion mobility of the 1,2,4-benzenetricarboxylate anion (1.45 $cm^2\ V^{-1}\ s^{-1}$), the reduced mobility of the strong feature in the 1,2,4,5-benzenetetracarboxylate spectra is seen to agree within 1.4%, which is well within experimental uncertainties. A similar situation is also observed when ions were drifting in CO_2. Here, the 1,2,4,5-benzenetetracarboxylate spectra contained only one feature corresponding to reduced mobility of 0.84 $cm^2\ V^{-1}\ s^{-1}$, which is identical (within the spectrometer resolution) to that of 1,2,4-benzenetricarboxylate anions. Considering both the structural similarity and large mass difference between these two carboxylate anions, it is hard to imagine that 1,2,4-benzenetricarboxylate anions and 1,2,4,5-benzenetetracarboxylate anions have the same mobility. Thus, it was concluded that 1,2,4-benzenetricarboxylate anions were generated through fragmentation of 1,2,4,5-benzenetetracarboxylate anions (i.e., decarboxylation) in these experiments to the point where the 1,2,4-benzenetricarboxylate anions were dominant in the N_2 spectra and the 1,2,4,5-benzenetetracarboxylate anions were undetected in the CO_2 spectra.

Neither the ESI process itself nor collisions with drift gas molecules in the IMS drift cell are energetic enough to cause fragmentation of the analyte ions. Previous studies of ESI−IMS have suggested that corona discharges can readily coexist with ESI sources operating in negative mode.[21] If a corona discharge is present at the tip of an operating ESI source, there is a strong likelihood that fragmentation of analyte ions will occur via collisions with energetic electrons of the corona. Therefore, the observed fragmentation of 1,2,4,5-benzenetetracarboxylate anion can most likely be attributed to the interaction with a corona discharge present at the tip of the ESI needle.

Plots of K_0^{-1} versus ion mass for carboxylate anions drifting in N_2 and CO_2 are shown in Figures 2 and 3, respectively, along with the best fit of the model to the measured data. Table 4 gives a tabulation of the modeled carboxylate anion mobilites in N_2 and CO_2 at masses corresponding to the ions considered in this work. Included in Table 4 are the values of the fitting

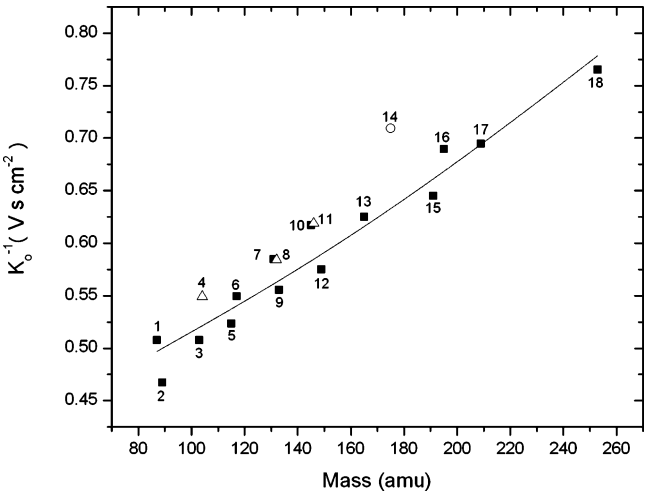

Figure 2. Plot of K_0^{-1} for carboxylate anions drifting in N_2 vs ion mass (solid squares). Deprotonated amino acid and ascorbic acid data are also shown as empty triangles and an empty circle, respectively. Each ion is labeled with the appropriate identifying number listed in Table 2. The solid line is the fit of the (12, 4) hard core potential model to the carboxylate data set ($r_0 = 2.51$ Å, $\gamma = 0.011$ Å/amu, $a^* = 0.2$).

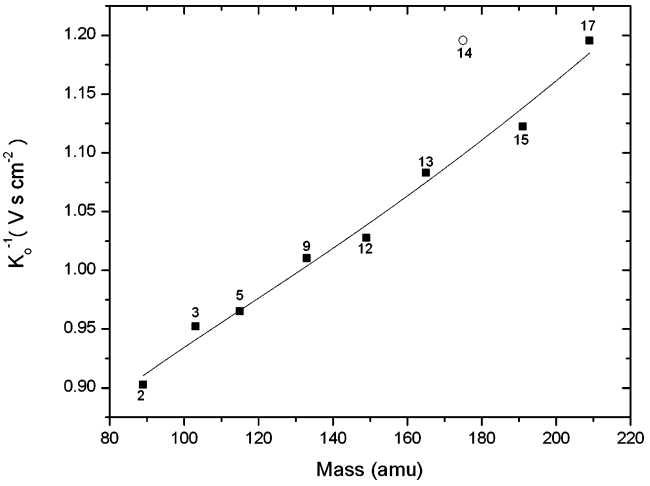

Figure 3. Plot of K_0^{-1} for carboxylate anions drifting in CO_2 vs ion mass (solid squares). The K_0^{-1} of deprotonated ascorbic acid is also shown as empty circle. Each ion is labeled with the appropriate identifying number listed in Table 2. The solid line is the fit of the (12, 4) hard core potential model to the carboxylate data set ($r_0 = 2.60$ Å, $\gamma = 0.011$ Å/amu, $a^* = 0.3$).

parameters that produced the optimum fits as well as the various physical properties of the ion−neutral system given by the model. All parameters returned by the model follow the same trends determined through similar modeling of protonated amino acids drifting in N_2 and CO_2.[9] Johnson et al.[9] have given a detailed discussion of these trends and their correlation with physical intuition of the ion−neutral interaction.

The worst observed deviation of the model from the mass−mobility data is 6.5%, with average deviations of 2.7% and 0.86% in N_2 and CO_2 drift gases, respectively. Such correlations are much better than the 20% level that is expected for structurally unrelated compounds.[10] Although the carboxylate anions studied here share a common, charge-carrying, carboxylate functional group, they otherwise exhibit a large degree of structural variation. This leads to the assertion that the common (charge-carrying) carboxylate functional group is the dominant factor in determining the mobilities of these compounds.

To examine this possibility further, ion mobilities were determined for other deprotonated organic acids and plotted along with the carboxylate anion data in Figures 2 and 3. Figure 2 shows mobilities of deprotonated serine, aspartic acid, glutaric acid, and ascorbic acid in N_2. Serine, aspartic acid, and glutaric acid show deviations from the modeled carboxylate mass−mobility correlation of only 5.4%, 3.8%, and 5.8%, respectively. These deviations are on the same order as the deviations between the measured carboxylate anions and the mass−mobility correlation model. Each of these amino acids is expected to be ionized through deprotonation of the carboxyl group and, therefore, share a common charge location with the carboxylate ions in this study. As a result, the demonstrated agreement with the modeled carboxylate mass−mobility correlation supports the assertion of the previous paragraph.

TABLE 4: Model Results for Carboxylate Anions Drifting in N_2 and CO_2

	N_2[b]				CO_2[c]			
MW[a]	K_0 (cm^2 V^{-1} s^{-1})	ϵ (meV)	r_m (Å)	Ω (Å^2)	K_0 (cm^2 V^{-1} s^{-1})	ϵ (meV)	r_m (Å)	Ω (Å^2)
87	2.059	3.697	8.62	87.3	1.101	13.47	8.11	139.1
89	2.047	3.539	8.71	87.7	1.096	12.91	8.19	139.2
103	1.959	2.638	9.38	90.1	1.060	9.730	8.79	140.6
115	1.888	2.085	9.94	92.4	1.033	7.753	9.31	142.1
117	1.877	2.008	10.0	92.8	1.028	7.474	9.39	142.3
131	1.799	1.554	10.7	95.8	0.999	5.835	9.99	144.5
133	1.789	1.500	10.8	96.2	0.995	5.639	10.1	144.8
145	1.727	1.221	11.4	99.0	0.970	4.619	10.6	147.0
149	1.707	1.143	11.6	99.9	0.962	4.331	10.8	147.7
165	1.632	0.884	12.3	103.7	0.930	3.378	11.5	151.1
191	1.521	0.600	13.6	110.1	0.879	2.318	12.6	157.5
195	1.505	0.567	13.8	111.1	0.871	2.194	12.8	158.6
209	1.452	0.468	14.5	114.7	0.845	1.818	13.4	162.5
253	1.309	0.267	16.6	126.0	0.766	1.053	15.3	176.5

[a] Molecular weight (amu). [b] $r_0 = 2.51$ Å $\gamma = 0.011$ Å/amu, $a^* = 0.2$. [c] $r_0 = 2.60$ Å, $\gamma = 0.011$ Å/amu, $a^* = 0.3$).

Ascorbic acid, which is expected to ionize via deprotonation of a hydroxyl group, shows a large deviation from the modeled carboxylate anion correlations in both N_2 and CO_2 (12% and 8.8%, respectively, see Figures 2 and 3). This expectation was confirmed with ESI−MS spectra of ascorbic acid samples that showed a dominant peak at *m*/*z* 175 (i.e., singly deprotonated ascorbate anions). However, there are four hydroxyl groups in ascorbic acid, each of which has the potential to be deprotonated. If the four ionic forms were in fact present during the experiments, and did not interconvert, one would expect multiple peaks in the IMS spectra. However, only a single feature was observed. Therefore, either one ionic form was dominant, or multiple forms were present that interconverted rapidly. Calculations of the optimized geometry of gas-phase ascorbate anions at the PM5 level show that deprotonation of the α-, β-, 5-, and 6-hydroxyl groups produce anions with heats of formation of −303, −315, −283, and −274 kcal/mol, respectively. These calculations indicate that the ascorbate anions formed via deprotonation of the β-hydroxyl group (i.e., the β-ionic form) are dominant in the gas phase and that interconversion among different ionic forms in our experiments was unlikely. The stability of the β-ionic form can be understood by charge delocalization from the remaining β oxygen to the carbonyl group. Because the charge-carrying functional group is different than the studied carboxylate anions, these observations further support the notion that charge location plays a key role in determining the relationship between an ion's mass and its mobility.

As mentioned earlier, a strong correlation between mass and mobility has previously been observed among protonated amino

TABLE 5: Heats of Formation, $\Delta_f H°$, Calculated for the Most Stable Extended and Cyclic (When Possible) Conformations of the Studied Carboxylate Anions Are Listed[a]

carboxylate anion	$\Delta_f H°$ for EC[b] (kcal/mol)	$\Delta_f H°$ for CC[c] (kcal/mol)	ring size in CC	$\Delta_r H°$ (kcal/mol)	$\Delta_r G°$ (kcal/mol)	E^c (kcal/mol)
pyruvate	−181.8					1.490
oxalate	−237.8					1.490
malonate	−236.9	−251.4	6	−14.5	−11.5	1.490
maleate	−219.5	−230.5	7	−11	−7.5	1.490
succinate	−245.1	−259.0	7	−13.9	−10.4	1.489
malate	−290.2	−303.7	7	−13.5	−10.0	1.489
tartarate	−339.2	−348.4	7	−9.2	−5.7	1.489
glutarate	−247.4	−261.8	8	−14.4	−7.5	1.489
adipate	−253.4	−266.6	9	−13.2	−6.3	1.489
phthalate	−210.8	−219.0	7	−8.2	−4.7	1.489
citrate	−392.1	−401.6	7	−9.5	−6.0	1.489
gluconate	−391.3					1.489
1,2,4-benzenetricarboxylate	−304.1	−312.5	7	−8.4	−4.9	1.489
1,2,4,5-benzenetetracarboxylate	−399.3	−405.1	7	−5.8	−2.3	1.489

[a] Reaction energies, $\Delta_r H°$, and subsequent free-energy changes, $\Delta_r G°$, for anions going from their cyclic to extended conformations are given along with the mean relative collision energies, E, for each anion under current experimental conditions. [b] Extended conformation. [c] Cyclic conformation.

acids which, like the carboxylate anions in this study, exhibit a high degree of structural variation.[9] Similar to the previous discussion, this work concluded that a common charge location on the amine groups was one of the dominant factors in determining the mobilities of protonated amino acids. It was further speculated that, in the gas phase, protonated amino acids could form intramolecular hydrogen-bonded ring structures between the amine and carboxyl groups. The stability of such structures could then help to ensure that the charge remains fixed on the common ring structure and thereby bring about the observed mass mobility correlation. The possibility of hydrogen-bonded ring structures forming in gas-phase muticarboxylate anions has been investigated through the computational modeling described in Section 4.

Calculated heats of formation, Δ_f H°, for the studied caboxylate anions are listed in Table 5 for the most energetically favorable extended conformations as well as the most energetically favorable cyclic conformations for carboxylates which can form H-bonded ring structures. As seen from Table 5, for all the carboxylate anions under investigation which can assume cyclic confomations, the cyclic confomations are the most energetically favorable, with the exception of oxalate. Such stable intramolecular hydrogen bond formation of dicarboxylate ions in vacuo has previously been reported by Aplin et al.[22] Hydrogen bonds that are formed between an acid and its conjugated base, such as the O−H···O$^-$ bonds considered here, can be classified as "very strong" hydrogen bonds.[23] Such bonds exhibit bond energies in the range of 15−40 kcal/mol and are quasicovalent in nature. Molecules that contain functional groups which can form such bonds always do so, unless there are adverse steric factors preventing their formation, as in the case of oxalic acid in the present study.

To assess the stability of the hydrogen-bonded ring structures at the temperatures and pressures found in the IMS drift cell, the free-energy changes, $\Delta_r G°$, between the most energetically favorable extended and cyclic conformations are compared with the mean relative collision energies. Free-energy changes were calculated on the basis of the law of compensation[24] as

$$\Delta_r G° = \Delta_r H° - T\Delta_r S° \tag{9}$$

and are listed in Table 5. To proceed, it was necessary to estimate values for $\Delta_r S°$. Benson[24] gives $\Delta_r S°$ between −3.8 and −5.2 cal mol^{-1} K^{-1} for open chains of n-C_4H_{10} through C_7H_{14}, forming four- through seven-membered hydrocarbon rings, while $\Delta_r S°$ is given as −9.1 cal mol^{-1} K^{-1} for n-C_8H_{18}, forming eight-membered rings. Meotner[25] gives $\Delta_r S°$ as −6.0 cal mol^{-1} K^{-1} and −7.0 cal mol^{-1} K^{-1} for intramolecular ring closure via ionic O−H$^+$···O bonds of 1,3-dimethoxypropane (six-membered ring) and 2,5-hexanedione (seven-membered ring), respectively, while $\Delta_r S°$ is given as −13.8 cal mol^{-1} K^{-1} for bis(2-methoxyethyl)ether, forming intramolecular H bond eight-membered rings. Therefore, $\Delta_r S°$ was taken to be −6.0, −7.0, and −13.8 cal mol^{-1} K^{-1} in the determination of $\Delta_r G°$ for carboxylates with cyclic conformations containing six, seven, and eight−nine members, respectively. These values were chosen, not only based on structural similarities with the compounds above, but also to provide "worst case" estimates of $\Delta_r G°$ for comparison with the experimental mean relative collision energies. The free-energy calculations show that it requires in excess of ∼1.0 to ∼10 kcal/mol to break the H bonds responsible for the cyclic conformations of the carboxylate anions and thereby transform the ions into their extended conformations.

Experimental mean relative collision energies can be determined from the Wannier energy formula,

$$E = \frac{1}{2}\mu v_r^2 = \frac{3}{2}kT + \frac{1}{2}Mv_d^2 \tag{10}$$

where E is mean relative collision energy, v_r is relative velocity, M is drift gas molecule mass, and v_d is drift velocity.[26] Under the current experimental conditions, eq 10 yields mean relative collision energies on the order of 1.5 kcal/mol. Comparison with the free-energy changes between cyclic and extended conformations of the anions under scrutiny shows that such collision energies are not sufficient to generate conformation changes. It is, therefore, concluded that the carboxylate anions studied here which form H-bonded rings exist primarily in their most stable cyclic conformations, as depicted in Figure 1. It is further noted that the charge on these ions will be located on the H-bonded ring structure.

Of note, the least energetic conformation of the citrate anion was a symmetric conformation that contained two intramolecular rings via H bonds between the neutral carboxyl groups and the carboxylate functional group. However, the energy difference between the symmetric conformation with two H-bonded intramolecular rings and that with a single H-bonded ring was only 1.3 kcal/mol. Therefore, the mean relative collision energies

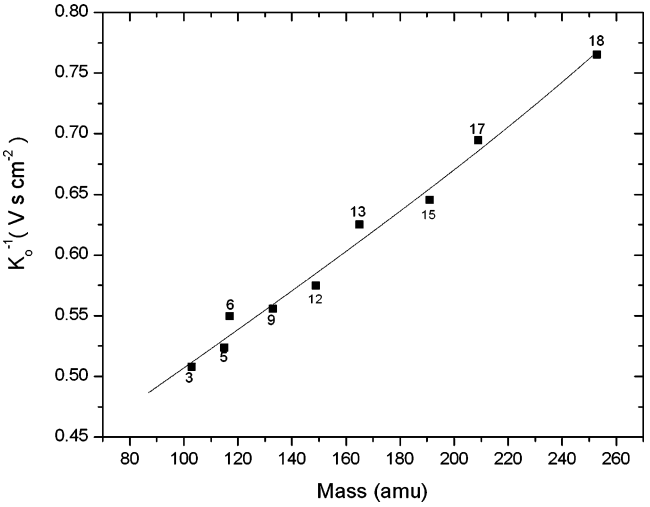

Figure 4. Plot of K_0^{-1} for carboxylate anions which assume planar-ring conformations drifting in N_2 vs ion mass (solid squares). Each ion is labeled with the appropriate identifying number listed in Table 2. The solid line is the fit of the (12, 4) hard core potential model to the solid squares ($r_0 = 2.51$ Å, $\gamma = 0.011$ Å/amu, $a^* = 0.2$).

within the drift cell (see Table 5) are sufficient to convert the anion from the two-ring symmetric conformation to the single-ring conformation depicted in Figure 1. Further, the H bond in the single-ring conformation is substantially stronger than the individual bonds in the two-ring conformation. As such, it was assumed that the single-ring conformation was the dominant conformation in the current experiments.

All the multicarboxylates studied here form relatively planar intramolecular hydrogen-bonded rings with the exception of glutarate and adipate, whose intramolecular hydrogen-bonded cyclic conformations are nonplanar. To examine whether the nature of the carboxylate conformations (planar-ring/nonplanar-ring/extended) affects the correlation between mass and mobility, beyond the common charge-carrying functional group, the (12, 4) potential model was fit to the mass−mobility data (in N_2) corresponding to carboxylates with planar-ring conformations. These data and model results are shown in Figure 4. As seen in the figure, there appears to be a better correlation among the planar-ring carboxylate subset than the studied carboxylates as a whole. The worst observed deviation of the model from the planar-ring mass−mobility data is 2.9%, with average deviations of 1.4%. This is, indeed, better agreement than when the entire data set was considered earlier. These results illustrate the role that structural similarities play in determining the mobilities of a given compound.

Of note, the carboxylate anions that form ring confirmations via intramolecular hydrogen bonding generally show higher K_0 values than those that form extended conformations. This is logical given that cyclic structures are more compact and would, therefore, be expected to have smaller collision cross sections than extended conformations.

6. Summary and Conclusions

ESI−IMS was used to study a variety of carboxylate anions. Reduced ion mobilities of the carboxylate anions were measured and were found to support the assertion that the identity of an ion's charge-carrying functional group plays an important role in determining the correlation between mass and mobility. In fact, the current observations suggest that charge location is the dominant factor in determining the degree of correlation between mass and mobility among a group of ions.

Computational analysis indicated that H-bonded ring conformations were energetically favored over extended conformations for all carboxylates studied that were capable of forming ring structures. Furthermore, it was found that such cyclic conformations would persist despite the collisions with neutral molecules at the temperatures and pressures corresponding to the current experimental conditions (500 K and 1 atm). Some evidence was seen that the subset of carboxylates which formed planar-ring structures demonstrated a better mass−mobility correlation than the data set as a whole.

A major objective of future missions to Mars will be to continue the search for organic molecules on the surface and subsurface. To accomplish this task, it is vital that the instruments onboard these missions are able to detect and uniquely identify organic compounds. An in situ tandem IMS−MS instrument would provide both the mass and mobility of sample analytes. This information would go a long way toward the goal of unique and unambiguous identification of the detected compounds. Further, the results published here, and elsewhere,[9] suggest that these data could be used to help identify charge-carrying structures and perhaps conformational properties of detected analytes based on correlations between mass and mobility among various compound classifications. Such information would provide an additional degree of robustness to compound identifications based on mass and mobility data.

Acknowledgment. This research was carried out at the Jet Propulsion Laboratory, California Institute of Technology, under a contract with the National Aeronautics and Space Administration (NASA) and at the Noyes Laboratory of Chemical Physics, California Institute of Technology. Financial support through NASA's Astrobiology Science and Technology Instrument Development, Planetary Instrument Definition and Development, and Mars Instrument Development programs is gratefully acknowledged. We appreciate critical discussion of Beauchamp group members, Heather A. Cox, Ronald L. Grimm, and Robert Hodyss through the whole research, and the support provided by the Mass Spectrometry Resource Center in the Beckman Institute. We also appreciate advice and discussion of Dr. Seung Soon Jang at the Materials Process Simulation Center, California Institute of Technology.

References and Notes

(1) Biemann, K.; Oro, J.; Toulmin, P.; Orgel, L. E.; Nier, A. O.; Anderson, D. M.; Simmonds, P. G.; Flory, D.; Diaz, A. V.; Rushneck, D. R.; Biller, J. A. *Science* **1976**, *194*, 72.

(2) Biemann, K.; Lavoie, J. M. *J. Geophys. Res.* **1979**, *84*, 8385.

(3) Flynn, G. J. *Earth, Moon, Planets* **1996**, *72*, 469.

(4) Hayatsu, R.; Anders, E. *Top. Curr. Chem.* **1981**, *99*, 1.

(5) Mullie, F.; Reisse, J. *Top. Curr. Chem.* **1987**, *139*, 83.

(6) Benner, S. A.; Devine, K. G.; Matveeva, L. N.; Powell, D. H. *Proc. Natl. Acad. Sci. U.S.A.* **2000**, *97*, 2425.

(7) Beegle, L. W.; Kanik, I.; Matz, L.; Hill, H. H. *Anal. Chem.* **2001**, *73*, 3028.

(8) Beegle, L. W.; Kanik, I.; Matz, L.; Hill, H. H. *Int. J. Mass Spectrom.* **2002**, *216*, 257.

(9) Johnson, P. V.; Kim, H. I.; Beegle, L. W.; Kanik, I. *J. Phys. Chem. A* **2004**, *108*, 5785.

(10) Griffin, G. W.; Dzidic, I.; Carroll, D. I.; Stillwell, R. N.; Horning, E. C. *Anal. Chem.* **1973**, *45*, 1204.

(11) Berant, Z.; Karpas, Z. *J. Am. Chem. Soc.* **1989**, *111*, 3819.

(12) Karpas, Z.; Berant, Z. *J. Phys. Chem.* **1989**, *93*, 3021.

(13) Asbury, G. R.; Hill, H. H. *J. Microcolumn Sep.* **2000**, *12*, 172.

(14) Wu, C.; Siems, W. F.; Asbury, G. R.; Hill, H. H. *Anal. Chem.* **1998**, *70*, 4929.

(15) Mason, E. A. In *Plasma Chromatography*; Carr, T. W., Ed.; Plenum Press: New York, 1984; Chapter 2.

(16) Eiceman, G. A.; Karpas, Z. *Ion Mobility Spectrometry*; CRC Press: Boca Raton, FL, 1994.

(17) Revercomb, H. E.; Mason, E. A. *Anal. Chem.* **1975**, *47*, 970.
(18) Mason, E. A.; O'Hara, H.; Smith, F. J. *J. Phys. B: At. Mol. Opt. Phys.* **1972**, *5*, 169.
(19) Berant, Z.; Karpas, Z.; Shahal, O. *J. Phys. Chem.* **1989**, *93*, 7529.
(20) Berant, Z.; Shahal, O.; Karpas, Z. *J. Phys. Chem.* **1991**, *95*, 7534.
(21) Asbury, G. R.; Hill, H. H. *Int. J. Ion Mobility Spectrom.* **1999**, *2*, 1.
(22) Aplin, R. T.; Moloney, M. G.; Newby, R.; Wright, E. *J. Mass Spectrom.* **1999**, *34*, 60.
(23) Desiraju, G. R.; Steiner, T. *The Weak Hydrogen Bond in Structural Chemistry and Biology*; Oxford University Press: New York, 1999.
(24) Benson, S. W. *Thermochemical Kinetics*; John Wiley & Sons: New York, 1976.
(25) Meotner, M. *J. Am. Chem. Soc.* **1983**, *105*, 4906.
(26) Wannier, G. H. *Bell Syst. Tech. J.* **1953**, *32*, 170.